Reprinted from THE REVIEW OF SCIENTIFIC INSTRUMENTS, Vol. 36. No. 11, 1540–1545, November, 1965
Printed in U. S. A.

Elastic Constants and Debye Temperature of TiC Using a New Ultrasonic Coherent Pulse/cw Technique

J. DE KLERK
Westinghouse Research Laboratories, Pittsburgh 35, Pennsylvania

(Received 7 June 1965)

A new simple but sensitive ultrasonic velocity measurement technique, using a coherent pulse/cw system, is described. The technique can readily be used for velocity measurements in either small or large samples, and does not require elaborate instrumentation. This technique has been used to measure the velocities of all three pure acoustic modes along a (110) direction of a single crystal of TiC. These velocities were then used to calculate the elastic constants and the Debye temperature for this sample. The measured velocities are $v_L=9.230\times10^5$ cm sec^{-1}, $v_{T_1}=6.425\times10^5$ cm sec^{-1}, and $v_{T_2}=5.927\times10^5$ cm sec^{-1}. The calculated elastic constants are $c_{11}=3.891\times10^{12}$ dyn cm^{-2}, $c_{12}=0.433\times10^{12}$ dyn cm^{-2}, $c_{44}=2.032\times10^{12}$ dyn cm^{-2}, and the room temperature Debye temperature is 935°K.

1. INTRODUCTION

TWO fairly recent comprehensive papers[1,2] have reviewed ultrasonic velocity measurement techniques employing either pulse or continuous wave (cw) techniques. The purpose of the present paper is to describe a technique which combines both methods, yet retains most advantages of each. Brief descriptions of the pulse echo and cw techniques are given in Secs. 2 and 3, respectively, to provide the background necessary to understand the coherent pulse/cw system described in Sec. 4. The instrumentation required for the new technique is described in Sec. 5. The relationship between acoustic velocities, elastic constants, and Debye temperature for cubic crystals is briefly reviewed in Sec. 6. The application of this technique to the measurement of the elastic constants and Debye temperature of a single crystal of titanium carbide is given in Sec. 7. A brief discussion of the advantages of this technique over other techniques is presented in Sec. 8. An Appendix is added giving the curves of intersection in the [x-y] and [110] planes of the velocity surface of TiC.

2. PULSE ECHO TECHNIQUE

The conventional ultrasonic pulse echo technique operates in the manner indicated in Fig. 1. A short burst of radio frequency electromagnetic energy (pulse) is applied to one side of a piezoelectric transducer which is acoustically bonded to one face of the sample material being studied. The rf electromagnetic pulse is converted by the piezoelectric transducer into mechanical energy which propagates in the sample at a velocity characteristic of the material. If the sample has been prepared in such a way that it has a second face parallel to and directly opposite the first face the mechanical pulse will echo back and forth between these two surfaces until all the mechanical energy has been dissipated in the sample. Each time the pulse returns to the first surface a small amount of the mechanical energy is converted by the piezoelectric transducer into electromagnetic energy, which is amplified and displayed on a cathode ray tube. The complete echo train appears as a series of evenly spaced pulses which decrease with time in an exponential manner.

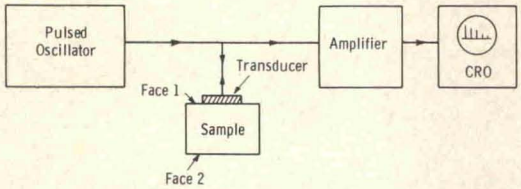

FIG. 1. Simplified block diagram of pulse echo system.

3. cw TECHNIQUE

The cw technique developed by Bolef and Menes[3,4] is operated by setting up mechanical standing waves in a composite oscillator, consisting of a piezoelectric transducer, an acoustic bond, and a sample identical to those employed in the pulse echo technique. A simplified block diagram of this system is shown in Fig. 2. The frequency ν of the Q-meter is adjusted so that a mechanical standing wave pattern near the resonant frequency ν_T of the transducer is generated in the composite oscillator. At this frequency a sharp minimum in the Q-meter reading is obtained.[4] The number of half wavelengths n of the mechanical standing wave system at this frequency ν_n is determined by the length ℓ_S of the sample and the velocity v_S of sound in the sample. The frequency of the Q-meter is next varied to obtain the frequencies $\nu_{(n-1)}$, $\nu_{(n-2)}$, . . . $\nu_{(n-m)}$, $\nu_{(n+1)}$, $\nu_{(n+2)}$, . . . $\nu_{(n+p)}$ for which there are

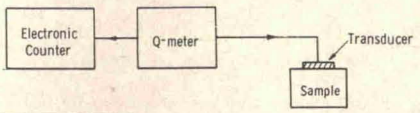

FIG. 2. Simplified block diagram of cw system.

[1] H. J. McSkimin, J. Acoust. Soc. Am. **33**, 606 (1961).
[2] D. I. Bolef and J. de Klerk, IEEE Trans. **UE-10**, 20 (1963).
[3] D. I. Bolef and M. Menes, Phys. Rev. **114**, 1441 (1959).
[4] D. I. Bolef and M. Menes, J. Appl. Phys. **31**, 1010 (1960).

respectively $(n-1)$, $(n-2)$, . . . $(n-m)$, $(n+1)$, . . . $(n+p)$ half-wavelengths in the mechanical standing wave system. If the mechanical Q for each of $(n-m)$ . . . $(n+p)$ mechanical resonances was calculated and plotted as a function of the standing wavenumber n, the plot shown in Fig. 3 would result. The average difference in frequency between two successive resonances, $\Delta\nu_{av}$, can be used to calculate the velocity of sound in the sample according to the formulae[2]

$$v=2\ell_S\Delta\nu_{av}(1+m_T/m_S), \tag{1}$$

or, more accurately, by

$$v=(2\ell_S/n)[\nu_n-(m_T/m_S)(\nu_T-\nu_n)], \tag{2}$$

where m_T and m_S are, respectively, the specific masses of transducer and specimen, ν_T is the resonant frequency of the transducer, and n is given by

$$n=[\nu_n/\Delta\nu_{av}][1-m_T/m_S]. \tag{3}$$

The most precise method of measuring ν_T has been developed by Breslow.[5] Briefly, this method uses a conventional pulse echo system[6] and a gated spectrum analyzer for determining the center frequency of successive echoes. When the driving frequency is below the resonant frequency ν_T, the center frequency of successive echoes increases until ν_T is reached and then remains constant. Likewise, when the driving frequency is greater than ν_T, the center frequency of successive echoes decreases until ν_T is reached and then remains constant. The value of ν_T required in Eq. (2) can be determined by tuning the transmitter until the center frequency of all the echoes, as determined by the spectrum analyzer, is the same. The frequency of the variable frequency oscillator (VFO) or transmitter is then measured by means of an electronic counter. The value of ν_T shown in Table I was not determined by the Breslow technique, but estimated from careful measurements of thickness of quartz, evaporated gold electrode, and bond, as a gated spectrum analyzer was not available.

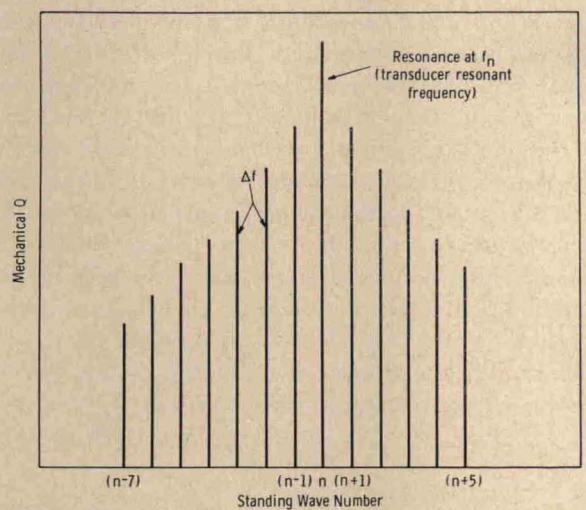

FIG. 3. Plot of mechanical Q vs standing wave number.

TABLE I. Frequency data for standing waves using v_L, v_{T_1}, and v_{T_2} modes.

Parameter	Propagation along [1$\bar{1}$0] for mode v_L	v_{T_1}	v_{T_2}
ν_n(Mc)	8.312566	8.203765	8.107342
$\Delta\nu_{av}$(Mc)	0.574014	0.403986	0.372672
ν_T(Mc)	7.903	7.987	7.987
Standing wavenumber n	14	20	21

4. COHERENT PULSE/cw TECHNIQUE

The cw system just described has the virtue of using the minimum of instrumentation, viz., only a Q-meter and an electronic counter. However, the correct operation of the Q-meter requires a great deal of patience and skill in obtaining accurate values of ν_n. It has been found possible to overcome this disadvantage by combining the pulse echo and cw techniques in the manner indicated in Fig. 4. If the variable rf attenuator and its connection to the matching network are disregarded, it will be seen that the remainder of the block diagram represents a conventional pulse echo system. The rf pulses are generated by coupling the output of a cw oscillator to a gated power amplifier instead of by the more frequently used self-excited oscillator.[6] This manner of generation is essential to achieve the coherence aspect of the new technique. With the variable rf attenuator disconnected, a normal pulse echo pattern is observed on the oscilloscope. By changing the VFO frequency the pulse echo pattern merely changes slightly in amplitude and decay rate. The maximum amplitude and minimum decay rate are simultaneously achieved by tuning the VFO frequency to coincide with the resonant frequency ν_T of the piezoelectric transducer. If a low level cw signal, obtained from the VFO via an rf attenuator, is

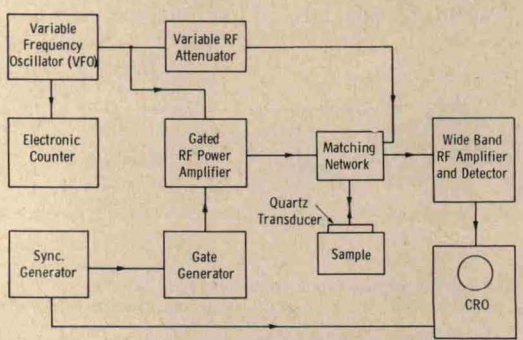

FIG. 4. Block diagram of pulse/cw system.

[5] D. H. Breslow, Report WAL 143/14-48 for Watertown Arsenal Contract DA-19-020-505-ORD-3882 (August 1956).

[6] B. Chick, G. Anderson, and R. Truell, J. Acoust. Soc. Am. 32, 186 (1960).

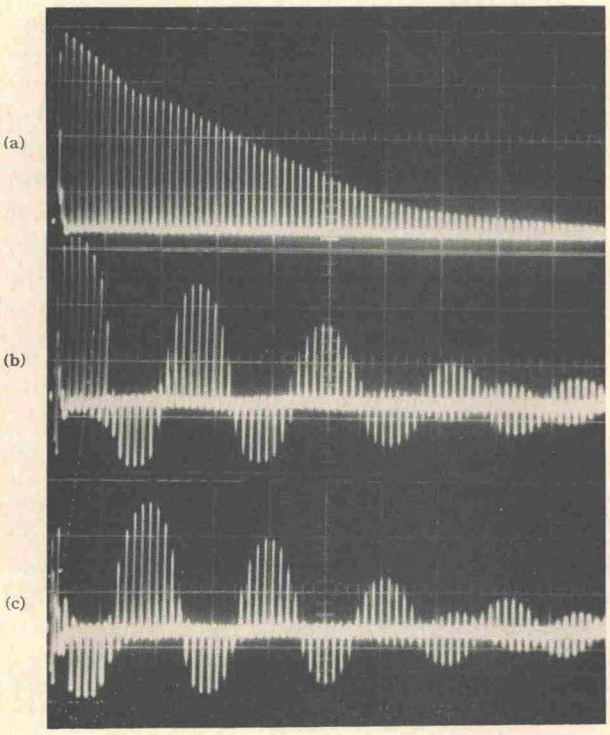

FIG. 5. Oscillogram of coherent pulse/cw signals.

now mixed with the pulse echo signal, interference between the two signals will occur. Constructive interference will result when the phase difference between the two signals is $r\pi$ radians, where r is an even integer. For all other phase differences, destructive interference will occur, maximum interference resulting when r is an odd integer. By adjusting the level of cw to approximately that of the early echoes in the pulse echo system and varying the frequency of the VFO, frequencies corresponding to $\nu_{(n-m)}$, . . . ν_n, . . ., $\nu_{(n+p)}$ of the cw technique can be found. These frequencies correspond to phase differences of $r\pi$ rad, where r is an even integer, that is when the pulse echo and cw signals are in phase. When the cw and pulse signals are out of phase, a sinusoidal modulation signal appears on the pulse echo envelope. The VFO frequency at which zero modulation occurs can rapidly be found with great accuracy by adjusting the VFO frequency and observing the pulse echo pattern. Figure 5 shows three oscillograms obtained when the VFO is tuned (a) to a frequency ν_n, for zero modulation, i.e., when the phase difference between pulse and cw signals is exactly $r\pi$ rad and r is an even integer; (b) to a slightly greater frequency $(\nu_n+\delta\nu)$ so that the phase difference is approximately 0.03 rad greater than $r\pi$; (c) to a slightly lower frequency $(\nu_n-\delta\nu)$, so that the phase difference is approximately 0.03 rad less than $r\pi$. For these oscillograms, $\nu_n=10.2202$ Mc, $\Delta\nu_{av}=0.1433$ Mc $\delta\nu\simeq 5$ kc. It should be noted that the nonsinusoidal modulation of the echo envelope of Fig. 5(a) is not due to the mixing of cw and pulse signals, but rather to the geometry of the sample and possibly to diffraction effects.[7] The greatest sensitivity in determining the frequencies for which the phase difference between pulse and cw signals is zero is achieved when the amplitude of the cw signal is made approximately equal to the amplitude of the early echoes in the pulse echo train as shown in Fig. 5.

The velocity of sound v can then be calculated using either Eq. (1) or Eqs. (2) and (3) of the cw method. Equation (1) can be simplified to

$$v=2\ell_S\Delta\nu_{av}, \tag{4}$$

if the accuracy of velocity measurement is required to within a few parts in 10^2. This method can only be adopted when $m_T/m_S<10^{-2}$.

5. INSTRUMENTATION

The equipment used in the coherent pulse/cw technique is shown in block diagram form in Fig. 4. Pulses of rf are generated by gating and amplifying the output of a VFO. The amplified rf pulses are coupled, via a matching network, to the quartz transducer, which is bonded to the sample. The matching network also serves to match the receiver to the transducer and to the cw rf source. The rf attenuator can be varied to adjust the level of cw signal being mixed with the pulse echo signals. The resultant signal is amplified by a wide band rf amplifier and subsequently detected before being displayed on a cathode ray tube. An electronic counter is used to measure the VFO frequency. A permanent record of the frequencies $\nu_{(n-m)}$, . . . ν_n, . . . $\nu_{(n+p)}$ can be obtained by using a digital printer coupled to the electronic counter.

Most of the units indicated in Fig. 4 are commercially available. Those used for the measurements described here are the following: General Radio unit oscillator type 1211B, Hewlett-Packard step attenuators types 355A and 355B, Beckman electronic counter type 7170, Beckman digital printer type 1453, Measurements Corporation pulse generator type 79B, Tektronix oscilloscope type 585. The

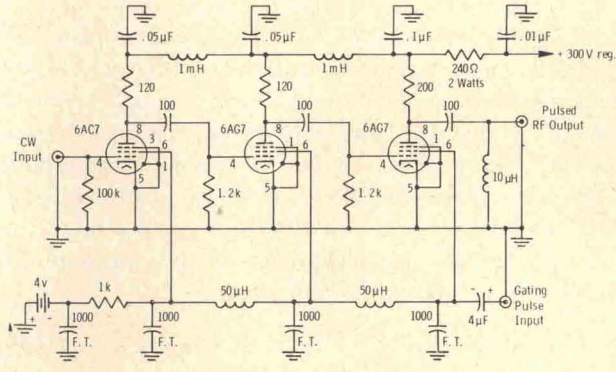

FIG. 6. Gated rf power amplifier.

[7] A. Seki, A. Granato, and R. Truell, J. Acoust. Soc. Am. **28**, 230 (1956).

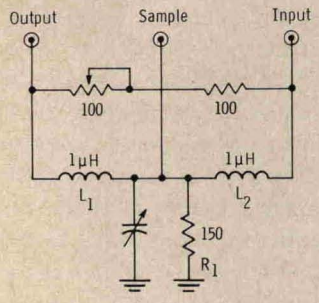

FIG. 7. Matching network.

wide band rf amplifier and detector was a modified surplus radar receiver. This unit can readily be replaced by a tuned commercial amplifier with a bandwidth of several megacycles and a gain of approximately 80 dB. The circuit of the gated rf power amplifier is shown in Fig. 6. The screen grid of each stage is held at a negative potential of 4 V. This bias is sufficient to hold each stage at cutoff. When a positive-going gating pulse of approximately 150 V is applied to the "gating pulse input" connector, all stages are simultaneously driven up to normal operating conditions, and the rf input signal is amplified for this short duration. Rejection of the cw signal between gating pulses is approximately 90 dB. This simple circuit provides adequate rf power when the maximum output from the VFO is coupled to the input. The circuit diagram of the matching network is given in Fig. 7. The network shown is for 20 Mc. L_1, L_2, and R_1 are switched to appropriate values when used at other frequencies. Connection to the cw source is made via a BNC T-connector to the "output" terminal.

6. RELATIONS BETWEEN ACOUSTIC VELOCITIES, ELASTIC CONSTANTS, AND DEBYE TEMPERATURE FOR CUBIC CRYSTALS

A strong analogy exists between the propagation of elastic and light waves in crystals, although the three surfaces—velocity, inverse, and wave—are considerably more complicated in the mechanical case. An expression of the condition for the existence of plane elastic waves in an anisotropic medium leads to a cubic equation in ρv^2, the elastic constants, and the direction of the wave normal, which yields three real positive roots for any value of (ℓ,m,n), the direction cosines of the wave normal. Associated with each velocity is a uniquely defined displacement vector, one quasilongitudinal and two quasitransverse. These three vectors form an orthogonal triad. The plot of $v(\ell,m,n)$ gives the velocity surface for any medium; for a cubic crystal the velocity equation is

$$H^3-aH^2+c(a+b)AH-c^2(a+2b)B=0, \qquad (5)$$

where $H=\rho v^2-c_{44}$; $a=c_{11}-c_{44}$; $b=c_{12}+c_{44}$; $c=c_{11}-c_{12}-2c_{44}$; $A=m^2n^2+n^2\ell^2+\ell^2m^2$; $B=\ell^2m^2n^2$; ρ is the density; v is the velocity.

In general, the normal to the wave surface does not coincide with the radius vector, or wave normal, and the propagation of energy takes place along three extraordinary rays; only when the wave normal and the normal to the wave surface coincide does the energy travel along the wave normal. A crystal of cubic symmetry possesses three such directions, viz., the [100], [110], and [111] types of direction. Hence, for propagation in the [100] direction, each ray is an ordinary ray, and as $\ell=1$, $m=n=0$, Eq. (5) yields the velocities

$$v_L=(c_{11}/\rho)^{\frac{1}{2}}, \qquad (6)$$

where v_L is the velocity of compressional waves and

$$v_{T_1}=v_{T_2}=(c_{14}/\rho)^{\frac{1}{2}}, \qquad (7)$$

where v_{T_1} and v_{T_2} are the velocities of the two shear waves.

For propagation in the [110] direction, each ray is an ordinary ray, as the wave normal and wave surface normal coincide. For this direction $\ell=m=1/\sqrt{2}$ and $n=0$ and Eq. (5) yields three unique velocities,

$$v_L=[(c_{11}+c_{12}+2c_{44})/2\rho]^{\frac{1}{2}}, \qquad (8)$$

$$v_{T_1}=(c_{44}/\rho)^{\frac{1}{2}}, \qquad (9)$$

$$v_{T_2}=[(c_{11}-c_{12})/2\rho]^{\frac{1}{2}}. \qquad (10)$$

For propagation in the [111] direction, $\ell=m=n=1/\sqrt{3}$ yielding the following velocities from Eq. (5),

$$v_L=[(c_{11}+2c_{12}+4c_{44})/3\rho]^{\frac{1}{2}}, \qquad (11)$$

$$v_{T_1}=v_{T_2}=[(c_{11}-c_{12}+c_{44})/3\rho]^{\frac{1}{2}}. \qquad (12)$$

Along this direction, the wave normal coincides with the normal to the compressional velocity surface, and hence energy propagates along the wave normal. The velocity of the shear waves is degenerate and consequently the displacement vectors are not uniquely defined, but may be in any direction contained by the plane of the wave. Also the normal to the velocity surface is not uniquely defined but may take up an infinity of positions, associated with different displacement vectors. This results in a cone of extraordinary rays giving rise to internal conical refraction.[8] The semi-angle of this cone is given by

$$\tan\Delta_c=c/(c+3c_{44})\sqrt{2}, \qquad (13)$$

where c is as defined for Eq. (5) and is the normal measure of the degree of elastic anisotropy possessed by a cubic crystal.

The Debye temperature θ can be evaluated from the equation[9]

$$\theta=(h/k)[3qN\rho/4\pi M]^{\frac{1}{3}}v_m, \qquad (14)$$

where h is Planck's constant, k is Boltzmann's constant,

[8] J. de Klerk and M. J. P. Musgrave, Proc. Phys. Soc. (London) **68B**, 81 (1955).
[9] O. L. Anderson, J. Phys. Chem. Solids **24**, 909 (1963).

TABLE II. Velocities and elastic constants derived from Eqs. (1), (2), and (4).

Computation equation used	Velocities along [1$\bar{1}$0] ($\times 10^5$ cm sec^{-1})			Elastic constants ($\times 10^{12}$ dyn cm^{-2})			Anisotropy ($\times 10^{12}$ dyn cm^{-2})
	v_L	v_{T_1}	v_{T_2}	c_{11}	c_{12}	c_{44}	$c=c_{11}-c_{12}-2c_{44}$
(4)	8.99	6.33	5.84	3.62	0.31	1.99	−0.68
(1)	9.219	6.419	5.921	3.881	0.429	2.029	−0.606
(2)	9.230	6.425	5.927	3.891	0.433	2.032	−0.606

N is Avogadro's number, M is the molecular weight, ρ is the density, q is the number of atoms per molecule, v_m is the averaged acoustic velocity.

The averaged acoustic velocity can be calculated from the expression

$$v_m=(\tfrac{1}{3}[2/V_T{}^3+1/V_L{}^3])^{-\frac{1}{3}}, \tag{15}$$

where V_L and V_T are, respectively, the averages of the compressional and shear acoustic velocities along the [100], [110], and [111] directions given above in Eqs. (6)–(12).

7. MEASUREMENTS

Velocity measurements by the coherent pulse/cw technique were made on a single crystal of TiC. Two suitable [1$\bar{1}$0] surfaces were ground and polished flat to $\lambda/4$ of sodium light and parallel to within 0.5′. The distance ℓ_S between these two polished faces was 0.7836 cm. A [110] orientation was chosen as the three independent velocities in this direction can be used in Eqs. (8), (9), and (10) and are adequate for calculating all three elastic constants c_{11}, c_{12}, and c_{44}, from which the velocities along the [100] and [111] directions may be computed. The velocities in all three directions are required for estimating v_m of Eq. (15). An X-cut quartz transducer, bonded to the sample by means of Canada balsam, was used to determine the compressional velocity. An AC-cut quartz transducer, bonded to the sample with Salol, was used for measuring both shear velocities, by first orienting the transducer polarization along the [110] and then the [001] direction. The pertinent parameters used in the computation of v_L, v_{T_1}, and v_{T_2} are given in Table I and Appendix I. The tabulated values of ν_n and $\Delta\nu_{\text{av}}$ are direct measurements recorded by the electronic counter, while n was calculated using Eq. (3). The data of Table I were used to calculate the velocities according to Eqs. (4), (1), and (2) and are listed in Table II. These values were then used to compute the elastic constants from Eqs. (8), (9), and (10). Table II lists these values together with values of the anisotropy c, computed from the definition of c for Eq. (5). The compressional and shear velocities in the [100] and [111] directions listed in Table III were calculated from Eqs. (6), (7), (11), and (12) using the elastic constants listed in Table II. The average velocities V_L and V_T were obtained from the velocities of Table III and used in Eq. (15) for obtaining the mean velocity v_m. This value of velocity was used to calculate the Debye temperature θ according to Eq. (14). The numerical values of the remaining parameters of Eq. (14) are listed in Appendix I. The velocities derived from Eqs. (1) and (2) are correct to within 10^{-3}, whereas the

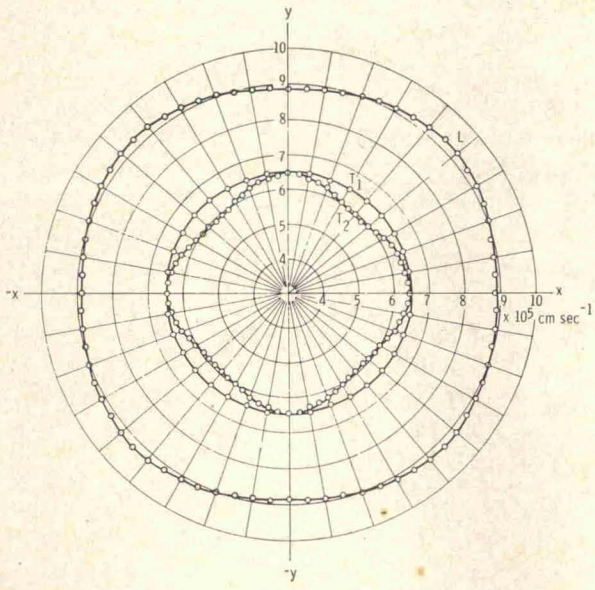

FIG. 8. Curves of intersection in (x-y) plane of velocity surface of TiC.

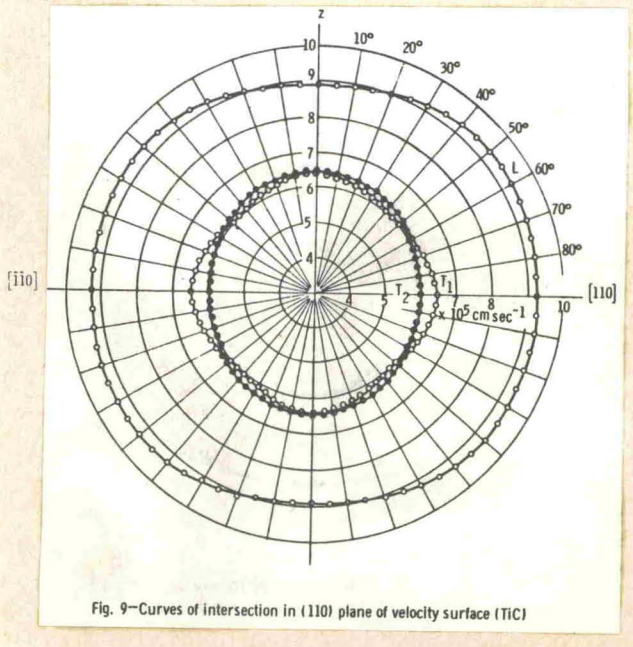

Fig. 9—Curves of intersection in (110) plane of velocity surface (TiC)

TABLE III. Velocities and Debye temperatures derived from Eqs. (1), (2), and (4).

Computation equation used	Measured velocities [1$\bar{1}$0] ($\times 10^5$ cm sec^{-1}) v_L	v_{T_1}	v_{T_2}	Calculated velocities [100] ($\times 10^5$ cm sec^{-1}) v_L	$v_{T_1}=v_{T_2}$	Calculated velocities [111] ($\times 10^5$ cm sec^{-1}) v_L	$v_{T_1}=v_{T_2}$	Mean velocity ($\times 10^5$ cm sec^{-1}) v_m	Debye θ °K
(4)	8.99	6.33	5.84	8.55	6.37	9.10	6.01	6.69	920
(1)	9.219	6.419	5.921	8.878	6.419	9.330	6.092	6.787	934
(2)	9.230	6.425	5.927	8.890	6.424	9.369	6.096	6.795	935

value of v_L derived from Eq. (4) is less than the true value by 2.5% and those of v_{T_1} and v_{T_2} by 1.5% as the end effect of the transducer is neglected in this equation. These values have been included to indicate the magnitudes of the errors introduced in the derived values of velocities, elastic constants and Debye temperature by neglecting the end effect of the transducer (see also Appendix II). The semi-angle of the cone of refraction of shear waves along the [111] direction is 4.5° according to Eq. (13). A more exact value of the mean velocity v_m of Eq. (15) can be derived from Figs. 8 and 9 as shown in Appendix II. This leads to a value of Debye temperature slightly lower than that given in Table III. However, these values are within 0.3% of each other. Thus the method used to determine the values of v_m given in Table III is justified for slightly anisotropic materials.

8. DISCUSSION

The coherent pulse/cw technique is a convenient, quick and fairly accurate method of determining the velocities, elastic constants, and Debye temperature of solids. By the use of an exponential waveform generator[5,10] the ultrasonic attenuation of the sample can be measured at the time the velocity measurements are being made. This method, while retaining the advantages of both pulse and cw techniques, avoids some of the disadvantages of each. The linearity of the CRO time base and the need for an accurate delay generator, which increase the complexity of the electronic instrumentation required for velocity measurement by conventional pulse echo techniques, as well as uncertainty in transit time measurement due to the presence of the transducer[11] are avoided in the coherent pulse/cw technique. The use of a wide band receiver and a variable attenuator in the latter technique, facilitates the rapid and accurate determination of mechanical resonance frequencies not possible with conventional cw systems even in the hands of a skilled operator.

[10] J. de Klerk, Ultrasonics 2, 137 (1964).
[11] E. W. Kammer, Report of NRL Progress, January 1965.

9. ACKNOWLEDGMENTS

The gated amplifier of Fig. 6 was designed by M. Menes and used by M. Menes and D. I. Bolef in their original work on the acoustic nuclear magnetic resonance technique.[3] The author would like to thank R. C. Kuzincki for orienting and F. N. Hauber for polishing the TiC crystal, and Miss Brenda J. Kagle for setting up the computer program used to obtain the data plotted in Fig. 9.

APPENDIX I

Density of quartz, $\rho_T=2.648$ g cm^{-3}

Density of TiC, $\rho_S=4.922$ g cm^{-3}

Length of sample, $\ell_S=0.7836$ cm

Ratio $m_{T_x}/m_S=0.0249$

Ratio $m_{T_{ac}}/m_S=0.0142$

$h=6.6251\times10^{-27}$ erg sec

$k=1.3805\times10^{-16}$ erg deg^{-1}

$N=6.0248\times10^{23}$ (g mole)$^{-1}$

$q=2$

$M=59.91$

APPENDIX II

Equation (5) has been used to derive the curves of intersection of the velocity surface of TiC in the [x-y] and [110] planes, by substitution of the measured values of c_{11}, c_{12}, and c_{44} and appropriate values of direction cosines ℓ, m, n in this equation. The results of this computation are given in Figs. 8 and 9, which indicate that the material is fairly isotropic, and hence the approximate method used in Sec. 7 for obtaining the mean velocity v_m is justified. A more exact determination of v_m based on the data presented in Figs. 8 and 9 is 6.756×10^5 cm sec^{-1}, which leads to a value of 930°K for the Debye temperature.